



## Original Article

## Brain Malformations Associated With Knobloch Syndrome—Review of Literature, Expanding Clinical Spectrum, and Identification of Novel Mutations



Ahmet Okay Caglayan MD<sup>a,b,c,\*</sup>, Jacob F. Baranoski<sup>a,b,c</sup>, Fesih Aktar MD<sup>d</sup>, Wengi Han PhD<sup>e</sup>, Beyhan Tuysuz MD<sup>f</sup>, Aslan Guzel MD<sup>g,h</sup>, Bulent Guclu MD<sup>i</sup>, Hande Kaymakcalan MD<sup>j</sup>, Berrin Aktekin MD<sup>k</sup>, Gozde Tugce Akgumus MS<sup>a,b,c</sup>, Phillip B. Murray MS<sup>a,b,c</sup>, Emine Z. Erson-Omay PhD<sup>a,b,c</sup>, Caner Caglar MS<sup>a,b,c</sup>, Mehmet Bakircioglu MS<sup>a,b,c</sup>, Yildirim Bayezit Sakalar MD<sup>l</sup>, Ebru Guzel MD<sup>m</sup>, Nihat Demir MD<sup>n</sup>, Oguz Tuncer MD<sup>n</sup>, Senem Senturk MD<sup>o</sup>, Baris Ekici MD<sup>p</sup>, Frank J. Minja MD<sup>q</sup>, Nenad Šestan<sup>e</sup>, Katsuhito Yasuno PhD<sup>a,b,c</sup>, Kaya Bilguvar MD<sup>c,r</sup>, Huseyin Caksen MD<sup>s</sup>, Murat Gunel MD<sup>a,b,c</sup>

<sup>a</sup> Department of Neurosurgery, Yale School of Medicine, New Haven, Connecticut

<sup>b</sup> Department of Neurobiology, Yale School of Medicine, New Haven, Connecticut

<sup>c</sup> Department of Genetics, Yale School of Medicine, New Haven, Connecticut

<sup>d</sup> Department of Pediatrics, Diyarbakir State Hospital, Diyarbakir, Turkey

<sup>e</sup> Kavli Institute for Neuroscience, Yale University School of Medicine, New Haven, Connecticut

<sup>f</sup> Division of Genetics, Department of Pediatrics, Istanbul University, Cerrahpasa Faculty of Medicine, Istanbul, Turkey

<sup>g</sup> Department of Neurosurgery, Bahcesehir University, Istanbul, Turkey

<sup>h</sup> Department of Neurosurgery, Medical Park Hospital, Gaziantep, Turkey

<sup>i</sup> Department of Neurosurgery, Sevkett Yilmaz Education and Research Hospital, Bursa, Turkey

<sup>j</sup> Department of Genetics and Bioinformatics, Bahcesehir University, Istanbul, Turkey

<sup>k</sup> Department of Neurology, Akdeniz University Medical Faculty, Antalya, Turkey

<sup>l</sup> Department of Ophthalmology, Faculty of Medicine, Dicle University, Diyarbakir, Turkey

<sup>m</sup> Department of Radiology, Medical Park Hospital, Gaziantep, Turkey

<sup>n</sup> Department of Pediatrics, Yuzuncu Yil University, Van, Turkey

<sup>o</sup> Department of Radiology, Istanbul Medeniyet University Göztepe Education and Research Hospital, Istanbul, Turkey

<sup>p</sup> Department of Pediatrics, Istanbul University, Istanbul Medical Faculty, Istanbul, Turkey

<sup>q</sup> Department of Radiology, Yale School of Medicine, New Haven, Connecticut

<sup>r</sup> Yale Center for Genome Analysis, Orange, Connecticut

<sup>s</sup> Department of Pediatrics, Necmettin Erbakan University, Meram Medical Faculty, Konya, Turkey

## ABSTRACT

**BACKGROUND:** Knobloch syndrome is a rare, autosomal recessive, developmental disorder characterized by stereotyped ocular abnormalities with or without occipital skull deformities (encephalocele, bone defects, and cutis aplasia). Although there is clear heterogeneity in clinical presentation, central nervous system malformations, aside from the characteristic encephalocele, have not typically been considered a component of the disease phenotype. **METHODS:** Four patients originally presented for genetic evaluation of symptomatic structural brain malformations. Whole-genome genotyping, whole-exome sequencing, and confirmatory Sanger sequencing were performed. Using immunohistochemical analysis, we investigated the protein expression pattern of *COL18A1* in the mid-fetal and adult human cerebral cortex and then analyzed the spatial and temporal changes in the expression pattern of *COL18A1* during human cortical development using the Human Brain Transcriptome

## Article History:

Received July 21, 2014; Accepted in final form August 28, 2014

\* Communications should be addressed to: Dr. Caglayan; Department of Neurosurgery; Yale School of Medicine; New Haven, Connecticut 06510.

E-mail address: [ahmet.caglayan@yale.edu](mailto:ahmet.caglayan@yale.edu)

database. **RESULTS:** We identified two novel homozygous deleterious frame-shift mutations in the *COL18A1* gene. On further investigation of these patients and their families, we found that many exhibited certain characteristics of Knobloch syndrome, including pronounced ocular defects. Our data strongly support an important role for *COL18A1* in brain development, and this report contributes to an enhanced characterization of the brain malformations that can result from deficiencies of collagen XVIII. **CONCLUSIONS:** This case series highlights the diagnostic power and clinical utility of whole-exome sequencing technology—allowing clinicians and physician scientists to better understand the pathophysiology and presentations of rare diseases. We suggest that patients who are clinically diagnosed with Knobloch syndrome and/or found to have *COL18A1* mutations via genetic screening should be investigated for potential structural brain abnormalities even in the absence of an encephalocele.

**Keywords:** Knobloch syndrome, cortical development, *COL18A1*, collagen XVIII, whole-exome sequencing

*Pediatr Neurol* 2014; 51: 806–813

© 2014 Elsevier Inc. All rights reserved.

## Introduction

First described by Knobloch and Layer in 1971,<sup>1</sup> Knobloch syndrome (OMIM: #267750, #608454) is a rare autosomal recessive syndrome characterized by stereotyped ocular abnormalities with or without occipital skull abnormalities. Ocular conditions traditionally include high myopia, lens subluxation, vitreoretinal degeneration, retinal detachment, and early-onset cataracts; occipital skull abnormalities can include encephalocele, bone defects, or cutis aplasia. Since the original report, at least 85 cases of Knobloch syndrome from 44 families have been described, each with varying degrees of clinical heterogeneity.<sup>2–5</sup>

In 2000, Sertie et al.<sup>6</sup> identified *COL18A1* (OMIM \*120328) as the disease-causing gene for Knobloch syndrome by performing linkage analysis in a large consanguineous family. The authors discovered a homozygous acceptor splice site mutation affecting the gene product of *COL18A1*. Since this original report, numerous mutations in *COL18A1* have been identified in unrelated families who have Knobloch syndrome, thus confirming its causal relation with the syndrome.<sup>7</sup> To date, more than 21 different mutations have been described in patients from various ethnicities.<sup>4–6,8–12</sup>

In addition to the characteristic ocular and occipital skull defects, Knobloch syndrome can present with a spectrum of phenotypic findings—some patients have presented with lung hypoplasia, hyperextensible joints, duplication of the renal collecting system, epilepsy, neuronal migration abnormalities, and dysmorphic findings such as midface hypoplasia, flat nasal bridge, dental abnormalities, high-arched palate, or micrognathia.<sup>10,13</sup>

Although neuronal migratory abnormalities and brain malformations have been previously reported in the literature (a total of seven patients from four case series, [Table 1](#)),<sup>3,9,10,14</sup> central nervous system malformations (aside from the characteristic encephalocele) have been considered relatively rare and have not traditionally been considered a hallmark feature of Knobloch syndrome. Here we describe four patients with structural brain malformations (with or without encephaloceles) who were found to possess frame-shift homozygous mutations in *COL18A1* via whole-exome and Sanger sequencing. When we further investigated these patients and their families, we discovered that these patients possessed some of the characteristic phenotypic features of Knobloch syndrome.

## Materials and Methods

### Participants

The study protocol was approved by the Yale Human Investigation Committee (protocol number 0908005592). Institutional review board approvals for genetic and magnetic resonance imaging studies, along with written consent from all study participants, were obtained by the referring physicians at the participating institutions. All fetal human tissues were collected under guidelines approved by the Yale Human Investigation Committee (protocol number 0605001466).

Human fetal brains at 20 and 22 weeks of gestation were obtained from the Human Fetal Tissue Repository at the Albert Einstein College of Medicine (CCI number 1993-042).

### Genome-wide genotyping

Samples were analyzed using an Omni 1M Quad V1-0 B SNP chip and 610K Quad Bead Chips according to the manufacturer's protocol (Illumina).

### Exome capture and sequencing

NimbleGen 2.1M human exome array (Roche Nimblegen, Inc) was used to capture the exomes of all samples according to the manufacturer's protocol with certain modifications, as described previously.<sup>15</sup> Sequencing of the library was performed on HiSeq 2000 using a bar-coding technology allowing for six samples per lane. The Illumina pipeline version 1.8 was used for image analysis and base calling. These methods were previously described in detail.<sup>16</sup>

### Exome data analysis

Analysis of the sequencing data was performed according to the previously described in-house written data analysis pipeline.<sup>17</sup> Briefly, we used sequence reads that passed Illumina quality filter for analyzing whole-exome data. We aligned reads to the human genome reference sequence (version GRCh37, the same as used in the phase 1 of 1000 Genomes Project) using Stampy (version 1.0.16)<sup>18</sup> in a hybrid mode with BWA (version 0.5.9-r16).<sup>19</sup> We detected variant sites (point mutations and small indels) using the Unified Genotyper algorithm from GATK.<sup>20</sup> We annotated variant alleles using Ensembl database (version 66) with the help of Variant Effect Predictor (v2.4) tool ([http://useast.ensembl.org/info/docs/variation/vep/vep\\_script.html](http://useast.ensembl.org/info/docs/variation/vep/vep_script.html)).

### Sanger sequencing

Coding regions and exon-intron boundaries of *COL18A1* were evaluated via Sanger sequencing using standard protocols. Amplicons were cycle sequenced on ABI 9800 Fast Thermocyclers, and post-cycle sequencing cleanup was carried out with CleanSEQ System (Beckman Coulter Genomics). The amplicons were analyzed on 3730×L DNA Analyzer (Applied Biosystems Inc).

**TABLE 1.**  
Summary of the Seven Previously Reported Patients With Knobloch Syndrome and Associated Brain Malformations

Clinical Feature	Kliemann et al., <sup>9</sup> Patient 2	Kliemann et al., <sup>9</sup> Patient 4	Paisán-Ruiz et al., <sup>14</sup> Patient 1	Paisán-Ruiz et al., <sup>14</sup> Patient 2	Khan et al., <sup>3</sup> Patient 1	Keren et al., <sup>10</sup> Patient 1	Keren et al., <sup>10</sup> Patient 2
Sex/age (yr)	M/7	F/13	F/47	F/41	M/12	F/5	M/17 wk of gestation
Ophthalmologic findings							
High myopia/severe visual loss	Yes	Yes	Yes	Yes	Yes	Yes	Not accessed; pregnancy terminated
Vitreoretinal/myopic degeneration	Yes	Yes	Yes	Yes	Yes	Yes	Not appreciated
Lens subluxation	No	No	Yes	Yes	Yes	Yes	No
Occipital bone defect/encephalocele	Yes	Yes	No	No	Yes	Yes	Yes
Neurological findings							
Mental status	Normal	Normal	Developmental delay; cognitive decline	Developmental delay; cognitive decline	Developmental delay	Mild developmental delay	Not accessed; pregnancy terminated
Seizures	No	Yes	Yes	Yes	Yes	No	No
MRI findings							
Multiple subependymal nodules retrocerebellar arachnoid cyst; ventricular dilation		Pachygyria (right frontal lobe); subependymal nodule (right lateral ventricle); calcification of right parietal lobe; ventricular dilation	Polymicrogyria (bilateral frontal and temporal lobes); marked cerebellar atrophy; brainstem and supratentorial volume loss; slender spinal cord	Polymicrogyria (bilateral frontal and temporal lobes); cerebellar atrophy; brainstem and supratentorial volume loss; slender spinal cord	Heterotopic gray matter in lateral ventricles	Pachygyria and polymicrogyria (bilateral frontal lobes); agenesis of the septum pellucidum; heterotopic hypersignals (on T <sub>2</sub> -weighted images) along radial migration tracts	Complete agenesis of cerebellar vermis; abnormal formation of cerebellar hemispheres; hamartomatous lesion of the mesencephalic roof
COL18A1 mutation	c.4181G>A	c.4181G>A	c.3514-3515 delCT	c.3514-3515 delCT	c.355delG	c.3544+3A>C	c.3544+3A>C
Abbreviations: F = Female M = Male MRI = Magnetic resonance imaging							

### Immunohistochemistry

Cortices from human fetal brain (20 weeks after conception) were fixed in 4% paraformaldehyde and cut into sections using a vibratome. Free-floating sections were preincubated in 1% hydrogen peroxide solution (T.J. Baker) at room temperature for 20 minutes and recovered in phosphate-buffered saline (PBS). Sections were then preblocked in blocking solution containing 5% normal donkey serum (Jackson Immuno Research Laboratories), 1% bovine serum albumin, 0.1% glycine, 0.1% lysine, and 0.3% Triton X-100 in PBS for 1 hour at room temperature. After preblocking, sections were incubated in anti-human endostatin (goat, 1:40; AF1098; R&D Systems) diluted in blocking solution on a horizontal shaker at 4°C for 48 hours and then washed in PBS at room temperature to remove excessive primary antibody. Sections were then incubated with biotinylated secondary antibody (Donkey Anti-Goat IgG; Jackson ImmunoResearch) diluted in blocking solution for 2 hours at room temperature. After washing in PBS, sections were further incubated in avidin-biotin-peroxidase complex (Vectastain ABC Elite Kit; Vector Laboratories) for 1 hour at room temperature and washed three times in PBS. Peroxidase activity was developed using a DAB peroxidase substrate kit (Vector Laboratories). Sections were mounted on Superfrost Plus charged slides (Fisher Scientific), allowed to air dry, and then were coverslipped with Permount (Fisher Scientific) for later examination and imaging.

### Results

#### Patient descriptions

Four patients, two boys and two girls, with a median age of 13.5 years (range, 13–22 years), and their parents and

siblings from four distinct consanguineous Turkish families (NG133, NG1348, NG1426, and NG159) were enrolled in our study in accordance with the policies of and following the approval by our institutional review board ([Supplementary Fig 1](#)). These four patients originally presented for genetic evaluation of symptomatic structural brain malformations. All four patients were confirmed to have structural brain malformations and various ocular abnormalities ([Table 2](#)). Representative magnetic resonance imaging findings from these patients are shown in [Fig 1](#).

#### Genotyping and whole-exome sequencing

DNA was extracted from the blood samples from the four patients and their parents and siblings. Whole-genome genotyping was performed for three of these four families (NG133, NG1348, and NG1426) and identified shared homozygous segments (each >2.5 cM) and revealed an index of homozygosity consistent with a consanguineous union in each of these three families. We then performed whole-exome sequencing using NimbleGen SeqCap EZ and the Illumina HiSeq 2000 on the index patients from each of these three families (as previously described).<sup>16</sup> We achieved mean 20× coverage of 87%, 82%, and 84% for NG133-1, NG1348-1, and NG1426-1, respectively, of all targeted bases ([Supplementary Table 1](#)). This coverage was more than sufficient to identify homozygous variants with a high

**TABLE 2.**  
Summary of the Clinical Findings for Each of Our Four Patients

Patient Characteristic	NG133-1	NG1348-1	NG1426-1	NG159-2
Sex/age	M/22 yo	M/14 yo	F/13 yo	F/13 yo
Consanguinity				
Patient's parents were	First cousins	First cousins	First cousins	First cousins
General				
Developmental delay	No	Yes	Yes	No
Facial dysmorphisms	No	No	Synorphys	No
Head and neck				
Microcephaly	No	No	No	No
Eyes				
High myopia	No	No	Yes	No
Vitreoretinal degeneration	Yes (L)	No	Yes	No
Retinal detachment (childhood)	No	No	No	Yes (BL)
Congenital aphakia	No	Yes (BL)	No	No
Optic discs	Normal	Normal	Atrophic (R)	Normal
Glaucoma	No	Yes (R)	Yes (R)	No
Lens subluxation	Yes (L)	Aphakia (BL)	No	No
Vitreous attachment at disc	No	No	Yes (R)	No
Loss of vision	Yes (L)	Yes (BL)	Yes (R)	Yes (BL)
Nystagmus	No	No	Yes	No
Other	Phthisis bulbi (R)	Leukoma (R)	No	No
Skeletal, hair, and skin				
Skull				
Midline occipital bone defect	No	No	No	Yes
Hair				
Alopecia at the occipital defect	No	No	No	No
Skin				
Occipital dermal sinus tract	No	No	No	Yes
Neurological				
Cognitive decline	Yes	Yes	Yes	Yes
Cerebellar signs	No	No	Yes	No
Seizures	Yes	Yes	Yes	No
Cardiovascular system				
Cardiac structural abnormalities	No	Atrial septal defect	No	No
Genitourinary system				
Renal				
Duplication of collecting system	No	No	No	No
MRI findings	Polymicrogyria	Polymicrogyria	Polymicrogyria	Cerebellar Vermian Atrophy
COL18A1 mutation	c.4768_4769delCT p.Leu1590ValfsX72	c.2309_2310insC p.Gly773ArgfsX55	c.5195_5196insTGCC p.Ala1734CysfsX14	c.4768_4769delCT p.Leu1590ValfsX72
COL18A1 domain affected	Endostatin	Alpha-helix	Endostatin	Endostatin

## Abbreviations:

BL = Bilateral  
 F = Female  
 L = Left  
 M = Male  
 MRI = Magnetic resonance imaging  
 R = Right  
 yo = Years old

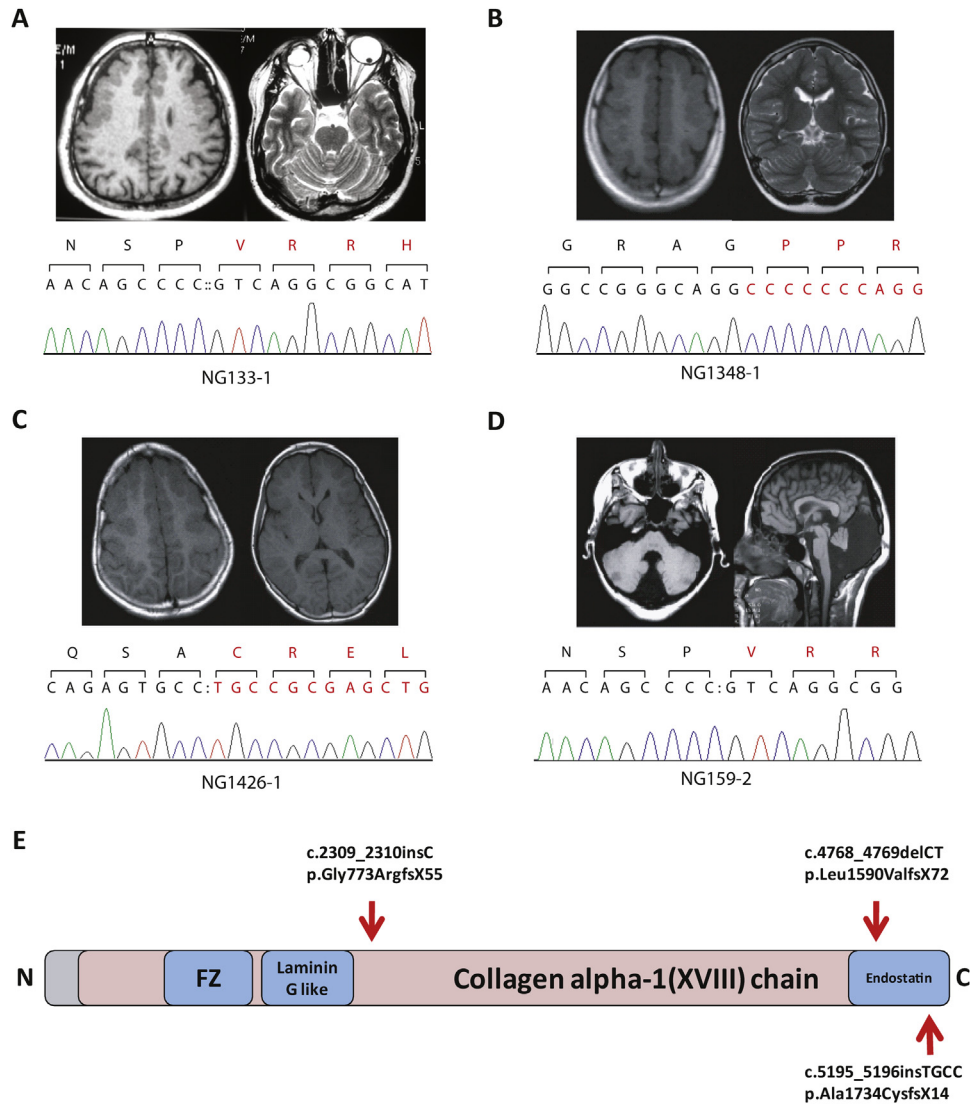
degree of specificity in each of these three patients (Supplementary Tables 2–4).

We identified two novel homozygous deleterious frame-shift mutations (c.2309insC [p.Gly773ArgfsX55] in NG1348-1 and c.5199\_5202insTGCC [p.Ala1734CysfsX14] in NG1426-1) and one previously reported mutation (c.4768\_4769delCT [p.Leu1590ValfsX72] in NG133-1) in the *COL18A1* gene (Table 3, Fig 1, and Supplementary Fig 2).<sup>14</sup> All variants were confirmed as homozygous in the affected patients and heterozygous in their respective parents via Sanger sequencing (Supplementary Fig 3). DNA extracted from Patient NG159-2's blood underwent Sanger screening for the exons of *COL18A1* and was found to harbor the homozygous c.4768\_4769delCT mutation (p.Leu1590ValfsX72). Like the other patients, NG159-2's parents were heterozygous for this variant (Supplementary Fig 4).

For two of the three patients who underwent whole-exome sequencing, we identified no other known disease-causing mutations that may have been responsible for their phenotypes. In Patient NG1348-1, we found a nonconserved missense mutation in *PCNT* in addition to the *COL18A1* mutation (Supplementary Table 3). However, although the mutation in *PCNT* may be contributing to the phenotype, we believe that it is the *COL18A1* mutation that is predominantly responsible for abnormalities identified in this patient.

*COL18A1* expression in the developing brain

To better understand the potential for mutations in *COL18A1* to contribute to the pathogenesis of central nervous system malformations in these patients, we assessed the extent to which *COL18A1* was expressed in the developing

**FIGURE 1.**

Magnetic resonance imaging findings for our four patients and schematic representation of the *COL18A1* gene and the mutation locations were given. For each mutation, representative chromatographs obtained via Sanger sequencing analysis of *COL18A1* patients. (A) Panels left and right—axial T<sub>1</sub>- and T<sub>2</sub>-weighted images, respectively, of Patient NG133-1 demonstrating polymicrogyria of the bilateral frontal lobes and evidence of vitreoretinal degeneration in the left eye globe with phthisis bulbi in the right eye globe, respectively. (B) Panels left and right—axial T<sub>1</sub>-weighted and coronal T<sub>2</sub>-weighted images, respectively, of Patient NG1348-1 demonstrating polymicrogyria involving the bilateral frontal and parietal lobes. (C) Panels left and right—axial T<sub>1</sub>-weighted images of Patient NG1426-1 indicating polymicrogyria in the bilateral frontal lobes. (D) Panels left and right—axial and sagittal T<sub>1</sub>-weighted images, respectively, of Patient NG159-2 illustrating a Dandy-Walker malformation (cerebellar vermian atrophy). There is also an occipital bony defect present without any visible herniation of the meninges or brain parenchyma. (E) Schematic representation of the *COL18A1* gene and the mutations identified in the described patients. (The color version of this figure is available in the online edition.)

brain. First, we performed immunohistochemistry using antibodies against endostatin, a naturally-occurring C-terminal fragment derived from *COL18A1*. We found that *COL18A1* protein is highly expressed in the pia and blood vessels of postmortem mid-fetal (Fig 2A) and adult (Fig 2B) human cerebral cortex, which is similar to the expression of *Col18a1* in the embryonic mouse brain (Fig 2C).

We then analyzed the spatial and temporal changes in the expression pattern of *COL18A1* during human cortical development using the Human Brain Transcriptome database.<sup>21</sup> The Human Brain Transcriptome database is a public database containing genome-wide RNA expression data, and associated metadata set was generated from 1340

tissue samples collected from 16 brain regions including the cerebellar cortex, mediodorsal nucleus of the thalamus, striatum, amygdala, hippocampus, and 11 areas of the neocortex of 57 developing and adult postmortem brains of clinically unremarkable donors representing males and females of multiple ethnicities. The relative levels of RNA expression can be tracked over the course of development. We found that *COL18A1* mRNA expression is low-to-moderate ( $6 < \log_2 \text{intensity} < 7$ ) in the cortical areas of human brains (Supplementary Fig 5).<sup>21</sup> We next performed co-expression analysis<sup>21,22</sup> on *COL18A1* and found that *COL18A1* is positively coexpressed with genes known to cause cortical malformation syndromes such as *DOCK6* (responsible for

**TABLE 3.**Summary of the Mutations Identified in *COL18A1* and the Resulting Protein Alterations in Each of Our Four Patients

Patient ID	Chr	Position Start	Position End	Position in CDS	Mutation	Result	Highest Impact Protein Change	COL18A1 Domain
NG133-1	21	46930004	46930005	c.4768_4769 delCT	“CT” deletion	Frame shift	p.Leu1590ValfsX72	Endostatin
NG1348-1	21	46897722	46897722	c.2309insC	“C” insertion	Frame shift	p.Gly773 ArgfsX55	Alpha-helix
NG1426-1	21	46932246	46932250	c.5199_5202 insTGCC	“TGCC” insertion	Frame shift	p.Ala1734CysfsX14	Endostatin
NG159-2	21	46930004	46930005	c.4768_4769 delCT	“CT” deletion	Frame shift	p.Leu1590ValfsX72	Endostatin

## Abbreviations:

CDS = Coding DNA sequence

Chr = Chromosome

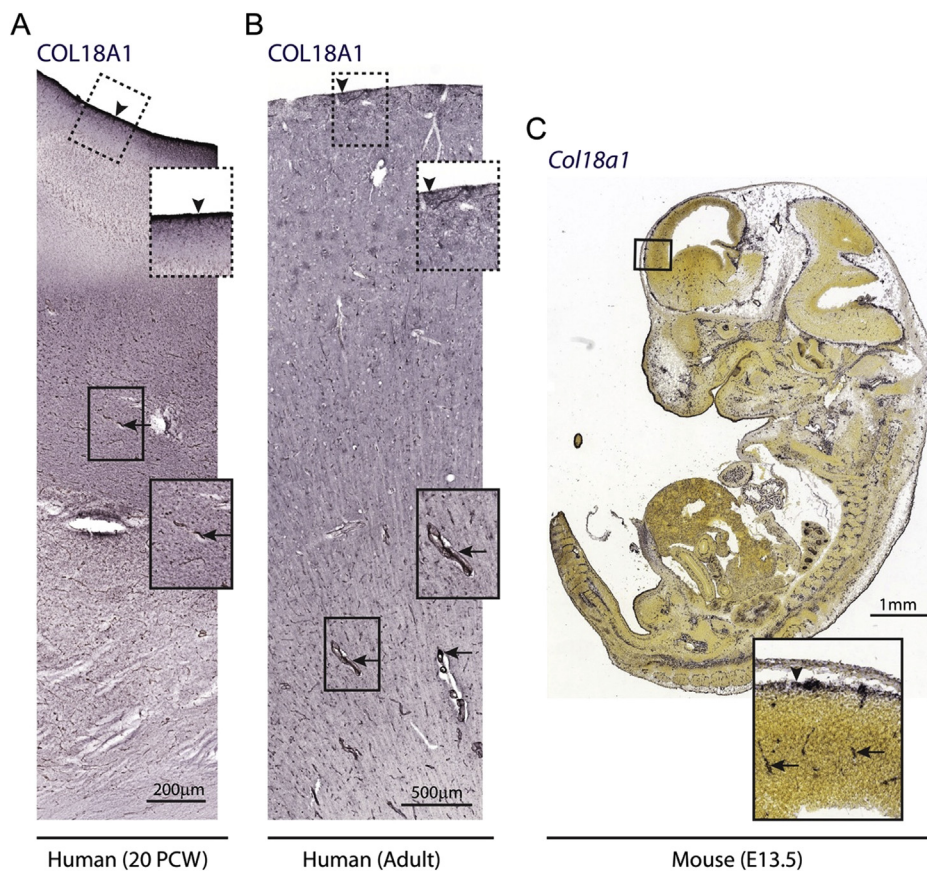
Adams-Oliver syndrome 2), *LAMC3* (responsible for occipital cortical malformations), and *COL6A3* (responsible for Bethlem myopathy) (Supplementary Table 5).

**Discussion***COL18A1 and Knobloch syndrome*

*COL18A1* is located on the long arm of chromosome 21 (chr21q22.3) and is composed of 43 exons. It encodes the collagen XVIII protein, which has been revealed to be an important component of basement membranes.<sup>23</sup> *COL18A1* has at least three distinct isoforms of different lengths;

these isoforms arise through the use of at least two promoters and alternative splicing in the third exon.<sup>24,25b</sup> Although *COL18A1* is ubiquitously expressed, its isoforms have different tissue and developmental distribution.<sup>7</sup> In addition to these three isoforms, *COL18A1* can produce endostatin via proteolytic cleavage. Endostatin is a signaling molecule known to inhibit the migration and proliferation of endothelial cells and is capable of suppressing angiogenesis.<sup>26</sup>

Genetic studies have identified exons 30 through 42 of *COL18A1* as being the most frequently mutated in Knobloch syndrome patients; however, there remains much heterogeneity in mutation site distribution.<sup>4</sup> Recently, germline

**FIGURE 2.**

In the mid-fetal (A) and adult (B) human cerebral cortex, *COL18A1* protein is expressed in the pia (arrow heads) as well as the blood vessels (arrows). In the mouse embryo (C), mouse *Col18a1* mRNA is also highly expressed in the cerebral cortex. Mouse images were obtained from the publicly available Allen Developing Mouse Brain Atlas (<http://developingmouse.brain-map.org/>). PCW, postconception weeks; E, embryonic day. Rectangles represent area displayed in magnified panels. (The color version of this figure is available in the online edition.)

compound heterozygous mutations were also described in patients with Knobloch syndrome.<sup>8</sup>

In our cohort of four patients, who presented with brain malformations, we identified two novel homozygous deleterious mutations and found one mutation that was previously reported<sup>14</sup>—all mutations were located in either the alpha-helix or the endostatin domains of *COL18A1* (Fig 1).

Aside from one patient (NG1348-1) who possesses a nonconserved missense mutation in *PCNT*, none of the four individuals described in this study possessed any other known disease-causing mutations that may have been responsible for their phenotypes. Patient NG1348-1 displayed none of the characteristic phenotypical findings associated with *PCNT* mutations (stereotyped facial dysmorphisms, microcephaly, long-bone and/or axial skeleton aberrations, high-pitched voice, microdontia, hyperinsulinism, pigmentation abnormalities, and so forth).<sup>27</sup> Although the mutation in *PCNT* may be contributing to the phenotype, the clinical presentation of this patient is much more consistent with a Knobloch syndrome diagnosis and suggests that it is the mutation in *COL18A1* that is responsible for the observed brain malformations.

#### *Clinical features of Knobloch syndrome*

Ocular and occipital skull defects are the two hallmark features of Knobloch syndrome. Ocular defects often appear before 1 year of age and include progressive high myopia, lens subluxation, vitreoretinal degeneration, retinal detachment, and cataracts.<sup>1,2,4</sup> All four patients in our cohort were evident to have ocular abnormalities consistent with the Knobloch syndrome phenotype.

Occipital skull defects range from encephaloceles to purely bone lesions to scalp abnormalities such as cutis aplasia.<sup>1,2,4</sup> Studies have found that there is no correlation between the size or the severity of occipital abnormality and the site of the mutation in *COL18A1*; our findings are consistent with these data. Further, variability in the size of the occipital alteration is commonly observed in both intrafamilial and interfamilial cases, and sometimes, it is noticed only through computed tomographic scan.<sup>2,7</sup> Interestingly, only one of the four patients in our cohort was evident to have an occipital defect characteristic of the Knobloch syndrome phenotype.

Although both early-onset high myopia and the presence of an occipital skull defect are the two hallmark clinical features of patients with Knobloch syndrome, a spectrum of phenotypic expressions clearly exists. Because of the variable presentation of occipital defects, we can assume that a certain percentage of patients who harbor mutations in *COL18A1* will present without any occipital skull abnormalities.

This may explain the lack of occipital skull phenotype in our patients. Further, a number of sporadic Knobloch syndrome patients who present with only ocular defects may go undiagnosed.<sup>9,28,29</sup> Given the consanguinity, a second disorder might also be possible although this should have been evident on exome sequencing with homozygous changes.

A recent study by Khan et al.<sup>3</sup> also demonstrated that ophthalmic findings are sufficient to accurately diagnose Knobloch syndrome. Therefore, an experienced

ophthalmologist is capable of properly diagnosing patients with this condition. This highlights the importance of the ocular phenotype and offers further evidence of the phenotypic heterogeneity of this disorder.

Interestingly, all our cases have cognitive decline and/or developmental delay, neither of which is common in Knobloch syndrome patients (Table 2). One possible explanation is previous studies have documented the high rates of concomitant developmental and neurological disability that are associated with structural brain disorders.<sup>30</sup> Severity and types of behavioral and cognitive outcomes of the structural brain disorders seem to be depending on the location of the cortical abnormality.<sup>31</sup> However, we believe that generally a precise diagnostic prediction of abnormalities associated with specific anomalies has not been possible, and this issue requires further studies.

We observed additional aberrations in our patients including atrial septal defects, seizures, and minor dysmorphic findings. These findings highlight the wide phenotypic spectrum that Knobloch syndrome can encompass and also further illustrates the importance of type XVIII collagen in the normal development of multiple organ systems.

#### *Brain malformations in Knobloch syndrome*

To date, only four case series describing a total of seven patients reported brain malformations associated with Knobloch syndrome (Table 1).<sup>3,9,10,14</sup> As with other phenotypic manifestations of Knobloch syndrome, it appears that structural brain abnormalities due to mutations in *COL18A1* have marked heterogeneity. An additional possibility is that, because of methodologic limitations, we are failing to detect the other causative variants driving the brain malformation phenotype. Given our findings, we remain confident that mutations in *COL18A1* can result in a brain malformation phenotype. The mutations we identified were located in either the alpha-helical or the endostatin domains. It appears that mutations in either of these domains are sufficient to result in a brain malformation phenotype.

#### *Possible role of COL18A1 in human neurodevelopment*

Using immunohistochemical and expression analyses we have demonstrated *COL18A1* expression in the pia and blood vessels of the developing human cerebral cortex. In *C. elegans*, inactivation of collagen XVIII results in improper neuronal cell migration.<sup>30</sup>

These findings may suggest a potential role for *COL18A1* in human neurodevelopment. Furthermore, aberrations in neuronal migration that result from *COL18A1* mutations may contribute to the pathogenesis and phenotypes observed in these patients.

#### **Conclusions**

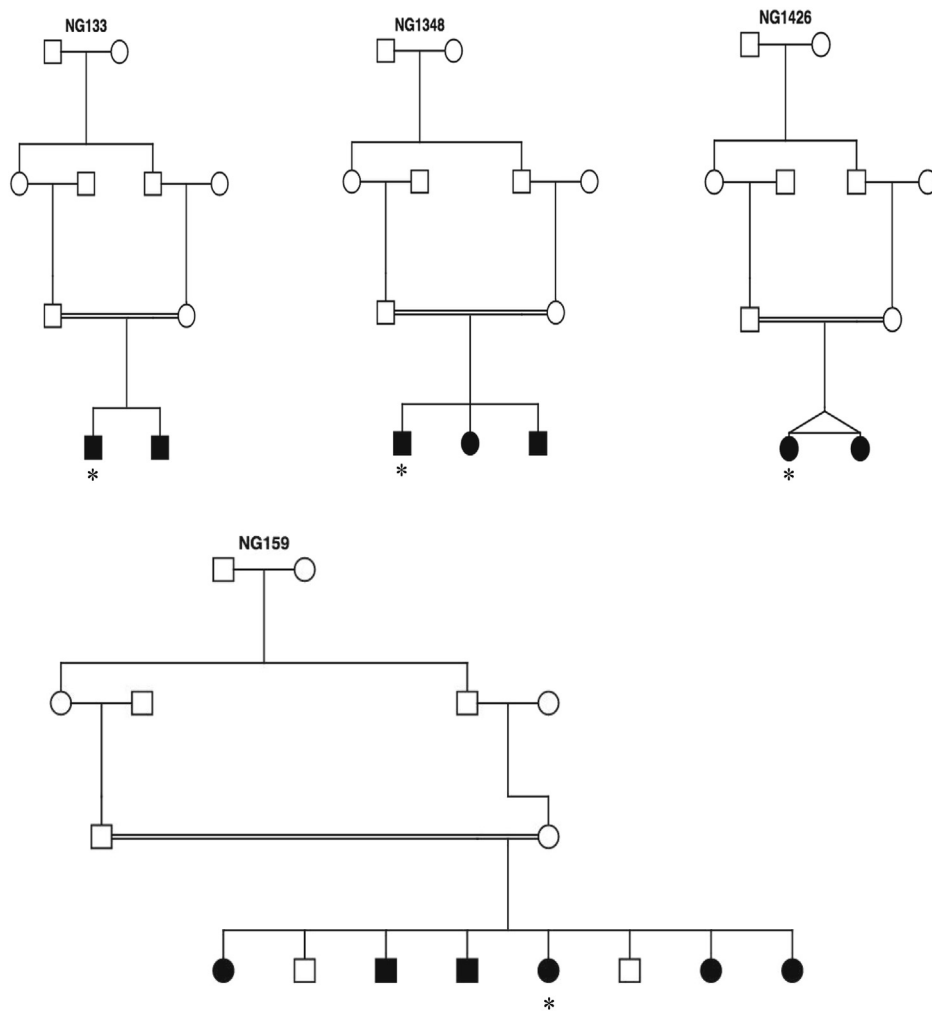
We describe a cohort of four patients from four consanguineous families who demonstrated phenotypic characteristics consistent with Knobloch syndrome and who were found to possess mutations in *COL18A1* via whole-exome and Sanger sequencing. All these patients presented with

various structural brain malformations aside from encephaloceles, an unusual finding for Knobloch syndrome. This study contributes to the reports demonstrating significant clinical variability in Knobloch syndrome while simultaneously highlighting the importance and persistence of the ocular phenotype. Furthermore, our data illustrate the intrafamilial and interfamilial phenotypic heterogeneity that can result from mutations in *COL18A1*—our genetic analysis and review of previously reported cases demonstrated no specific *COL18A1* isoform or mutation effect on the resulting phenotype. This report contributes to a better characterization of the brain malformations associated with deficiency of collagen XVIII, further elucidates potential Knobloch syndrome phenotypes, and suggests a role for *COL18A1* in cortical development. Finally, we propose that patients diagnosed with Knobloch syndrome and found to have *COL18A1* mutations should be investigated for potential central nervous system lesions.

The authors thank the patients and their families for participating in this study. The authors thank Angeliki Louvi, PhD for her contribution in editing the manuscript. This work was supported by the Yale Program on Neurogenetics and National Institutes of Health grants (RC2 NS070477 to M.G., U01MH081896 to N.S.), the Yale Center for Mendelian Disorders (U54HG006504 to R.P. Lifton, M.G., M. Gerstein, and S. Mane), the Howard Hughes Medical Institute (to W.H.), Gregory M. Kiez and Mehmet Kutman Foundation [to M.G.], and The Scientific and Technological Research Council of Turkey [2219 to A.O.C.].

## References

- Knobloch WH, Layer JM. Retinal detachment and encephalocele. *J Pediatr Ophthalmol*. 1971;8:181-184.
- Sniderman LC, Koenekoop RK, O'Gorman AM, et al. Knobloch syndrome involving midline scalp defect of the frontal region. *Am J Med Genet*. 2000;90:146-149.
- Khan AO, Aldahmesh MA, Mohamed JY, Al-Mesfer S, Alkuraya FS. The distinct ophthalmic phenotype of Knobloch syndrome in children. *Br J Ophthalmol*. 2012;96:890-895.
- Suzuki O, Kagae E, Bagatini K, et al. Novel pathogenic mutations and skin biopsy analysis in Knobloch syndrome. *Mol Vis*. 2009;15:801-809.
- Aldahmesh MA, Khan AO, Mohamed JY, et al. No evidence for locus heterogeneity in Knobloch syndrome. *J Med Genet*. 2013;50:565-566.
- Sertie AL, Sossi V, Camargo AA, Zatz M, Brahe C, Passos-Bueno MR. Collagen XVIII, containing an endogenous inhibitor of angiogenesis and tumor growth, plays a critical role in the maintenance of retinal structure and in neural tube closure (Knobloch syndrome). *Hum Mol Genet*. 2000;9:2051-2058.
- Suzuki OT, Sertie AL, Der Kaloustian VM, et al. Molecular analysis of collagen XVIII reveals novel mutations, presence of a third isoform, and possible genetic heterogeneity in Knobloch syndrome. *Am J Hum Genet*. 2002;71:1320-1329.
- Joyce S, Tee L, Abid A, Khaliq S, Mehdi SQ, Maher ER. Locus heterogeneity and Knobloch syndrome. *Am J Med Genet*. 2010;152A:2880-2881.
- Kliemann SE, Waetge RT, Suzuki OT, Passos-Bueno MR, Rosemberg S. Evidence of neuronal migration disorders in Knobloch syndrome: clinical and molecular analysis of two novel families. *Am J Med Genet*. 2003;119A:15-19.
- Keren B, Suzuki OT, Gerard-Blanluet M, et al. CNS malformations in Knobloch syndrome with splice mutation in *COL18A1* gene. *Am J Med Genet*. 2007;143A:1514-1518.
- Menzel O, Bekkeheien RC, Reymond A, et al. Knobloch syndrome: novel mutations in *COL18A1*, evidence for genetic heterogeneity, and a functionally impaired polymorphism in endostatin. *Hum Mutat*. 2004;23:77-84.
- Aldahmesh MA, Khan AO, Mohamed JY, et al. Identification of *ADAMTS18* as a gene mutated in Knobloch syndrome. *J Med Genet*. 2011;48:597-601.
- Passos-Bueno MR, Suzuki OT, Armelin-Correa LM, et al. Mutations in collagen 18A1 (*COL18A1*) and their relevance to the human phenotype. *An Acad Bras Cienc*. 2006;78:123-131.
- Paisan-Ruiz C, Scopes G, Lee P, Houlden H. Homozygosity mapping through whole genome analysis identifies a *COL18A1* mutation in an Indian family presenting with an autosomal recessive neurological disorder. *Am J Med Genet B Neuropsychiatr Genet*. 2009;150B:993-997.
- Choi M, Scholl UI, Ji W, et al. Genetic diagnosis by whole exome capture and massively parallel DNA sequencing. *Proc Natl Acad Sci U S A*. 2009;106:19096-19101.
- Bilguvar K, Ozturk AK, Louvi A, et al. Whole-exome sequencing identifies recessive *WDR62* mutations in severe brain malformations. *Nature*. 2010;467:207-210.
- Clark VE, Erson-Omay EZ, Serin A, et al. Genomic analysis of non-NF2 meningiomas reveals mutations in *TRAF7*, *KLF4*, *AKT1*, and *SMO*. *Science*. 2013;339:1077-1080.
- Lunter G, Goodson M. Stampy: a statistical algorithm for sensitive and fast mapping of Illumina sequence reads. *Genome Res*. 2011;21:936-939.
- Li H, Durbin R. Fast and accurate short read alignment with Burrows-Wheeler transform. *Bioinformatics*. 2009;25:1754-1760.
- DePristo MA, Banks E, Poplin R, et al. A framework for variation discovery and genotyping using next-generation DNA sequencing data. *Nat Genet*. 2011;43:491-498.
- Kang HJ, Kawasawa YI, Cheng F, et al. Spatio-temporal transcriptome of the human brain. *Nature*. 2011;478:483-489.
- Huang DW, Sherman BT, Lempicki RA. Systematic and integrative analysis of large gene lists using DAVID bioinformatics resources. *Nat Protoc*. 2009;4:44-57.
- Halfter W, Dong S, Schurer B, Cole GJ. Collagen XVIII is a basement membrane heparan sulfate proteoglycan. *J Biol Chem*. 1998;273:25404-25412.
- Saarela J, Rehn M, Oikarinen A, Autio-Harmainen H, Pihlajaniemi T. The short and long forms of type XVIII collagen show clear tissue specificities in their expression and location in basement membrane zones in humans. *Am J Pathol*. 1998;153:611-626.
- Saarela J, Ylikärppä R, Rehn M, Purmonen S, Pihlajaniemi T. Complete primary structure of two variant forms of human type XVIII collagen and tissue-specific differences in the expression of the corresponding transcripts. *Matrix Biol*. 1998;16:319-328.
- Schuch G, Heymach JV, Nomi M, et al. Endostatin inhibits the vascular endothelial growth factor-induced mobilization of endothelial progenitor cells. *Cancer Res*. 2003;63:8345-8350.
- Willems M, Genevieve D, Borck G, et al. Molecular analysis of pericentrin gene (*PCNT*) in a series of 24 Seckel/microcephalic osteodysplastic primordial dwarfism type II (MOPD II) families. *J Med Genet*. 2010;47:797-802.
- Knobloch WH, Layer JM. Clefting syndromes associated with retinal detachment. *Am J Ophthalmol*. 1972;73:517-530.
- Wilson C, Aftimos S, Pereira A, McKay R. Brief clinical report - Report of two sibs with Knobloch syndrome (encephalocele and vitreoretinal degeneration) and other anomalies. *Am J Med Genet*. 1998;78:286-290.
- Ackley BD, Crew JR, Elamaa H, Pihlajaniemi T, Kuo CJ, Kramer JM. The NC1/endostatin domain of *Caenorhabditis elegans* type XVIII collagen affects cell migration and axon guidance. *J Cell Biol*. 2001;152:1219-1232.
- Guerrini R, Parrini E. Neuronal migration disorders. *Neurobiol Dis*. 2010;38:154-166.

**SUPPLEMENTARY FIGURE 1.**

Pedigrees of the four consanguineous families. \* indicates the described index patients with brain malformations.

**NG133-1**

5'-CAGCCCCCTGTCAGGCGGCATGCGGGGCATCCGCGGGGCCGACTTCCAGTGCTTCCAGCAGGCGCG-3'  
 CAGCCCC\*\*GTCAGGCGGCATGCGGGGCATCCGCGGG  
 CAGCCCC\*\*GTCAGGCGGCATGCGGGGCATCCGCGGGGCCGA  
 CAGCCCC\*\*GTCAGGCGGCATGCGGGGCATCCGCGGGGCCGACTT  
 CAGCCCC\*\*GTCAGGCGGCATGCGGGGCATCCGCGGGGCCGACTTCCAGTGCT  
 CAGCCCC\*\*GTCAGGCGGCATGCGGGGCATCCGCGGGGCCGACTTCCAGTGCTTCC  
 CAGCCCC\*\*GTCAGGCGGCATGCGGGGCATCCGCGGGGCCGACTTCCAGTGCTTCCAGCAGGCGCG

**NG1348-1**

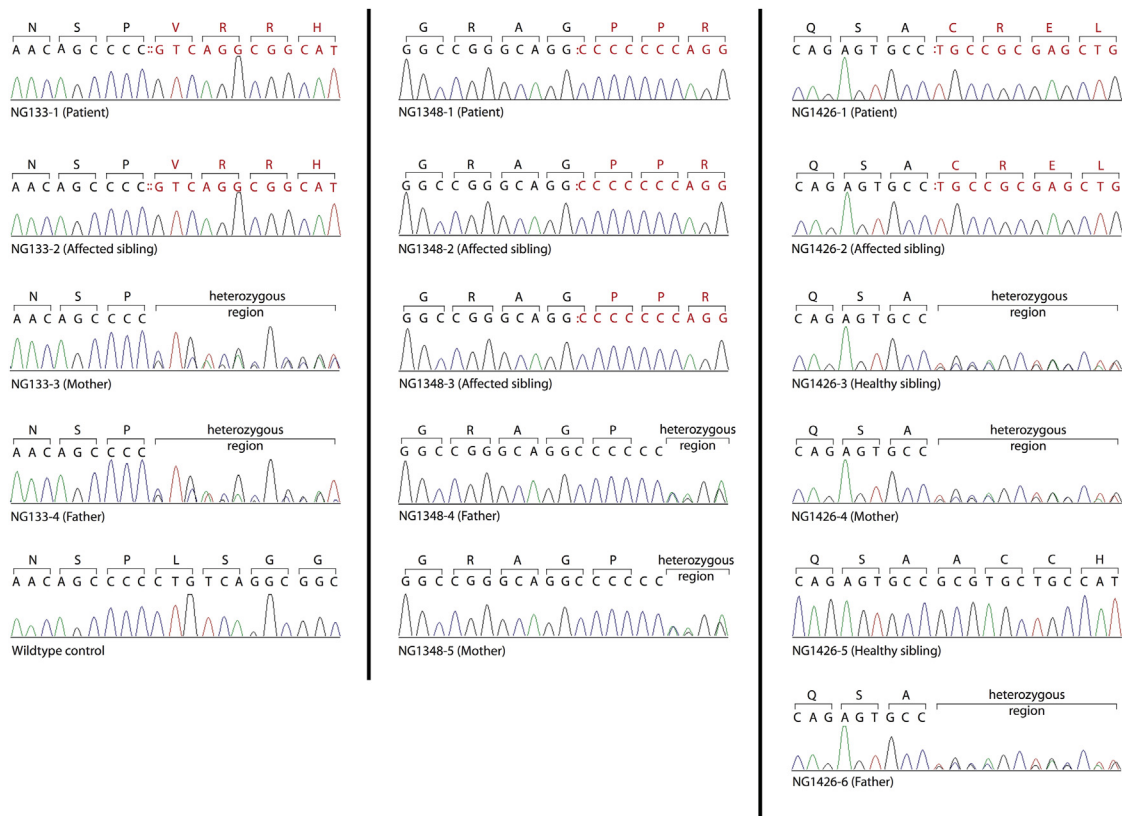
5'-GGGCAGG\*CCCCCAGGATCCCCATGCCTACCTGGTCCCCCGGGTCTCCCGTGC-3'  
 GGGCAGGCCCCCAGGATCCCCATGCCTACC  
 GGGCAGGCCCCCAGGATCCCCATGCCTACC  
 GGGCAGGCCCCCAGGATCCCCATGCCTACCTGGTCCC  
 GGGCAGGCCCCCAGGATCCCCATGCCTACCTGGTCCCCCGGGTCTCCCGTGC  
 GGGCAGGCCCCCAGGATCCCCATGCCTACCTGGTCCCCCGGGTCTCCCGTGC  
 GGGCAGGCCCCCAGGATCCCCATGCCTACCTGGTCCCCCGGGTCTCCCGTGC  
 GGGCAGGCCCCCAGGATCCCCATGCCTACCTGGTCCCCCGGGTCTCCCGTGC

**NG1426-1**

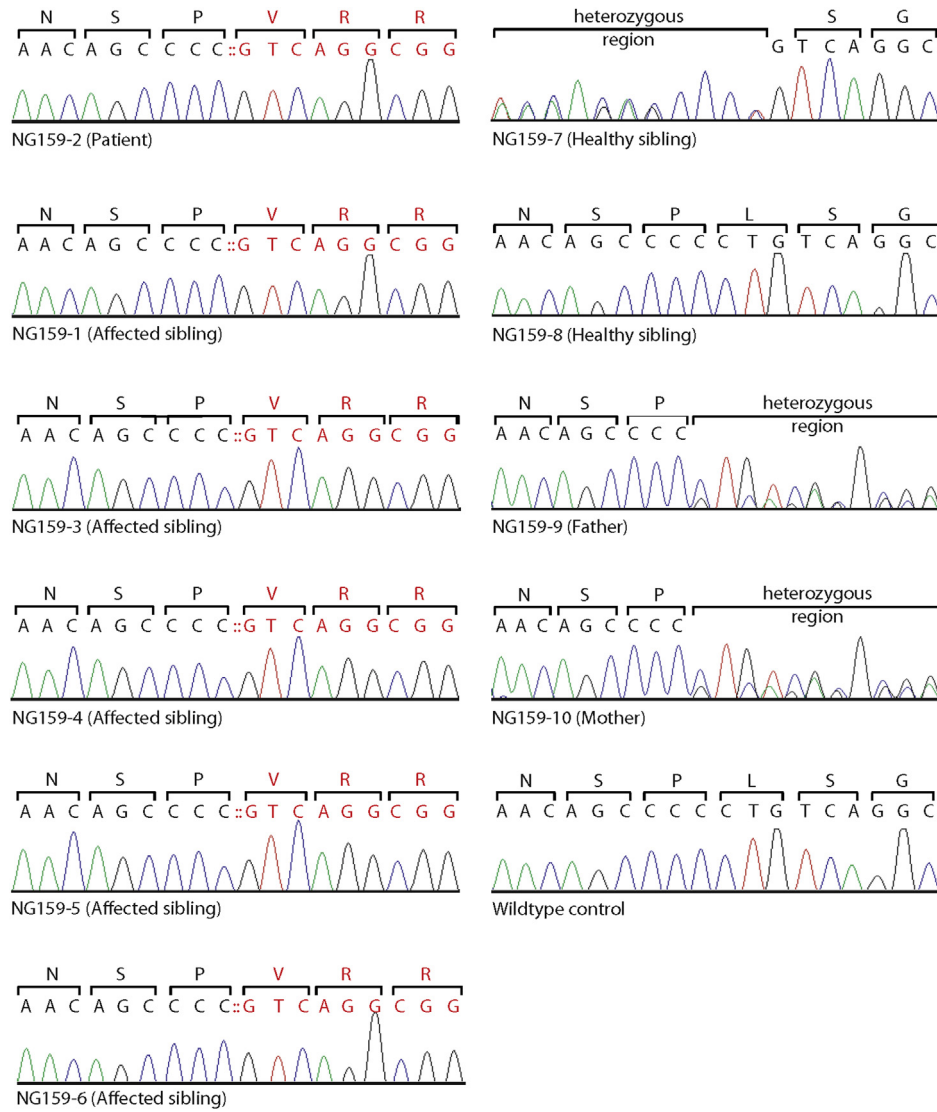
5'-GGCAGAGTGCC\*\*\*\*GCGAGCTGCCATCACGCCTACATCGT-3'  
 GGCAGAGTGCTGCCGCGAGCTGCCATCAC  
 GGCAGAGTGCTGCCGCGAGCTGCCATCACGCC  
 GGCAGAGTGCTGCCGCGAGCTGCCATCACGCCTAC  
 GGCAGAGTGCTGCCGCGAGCTGCCATCACGCCTACATC

**SUPPLEMENTARY FIGURE 2.**

Alignment data for the three index patients analyzed via whole-exome sequencing (NG133-1, NG1348-1, and NG1426-1) demonstrating the identified mutations in *COL18A1*. The top line in each panel represents the nonmutated reference sequence. The subsequent lines below the reference lines depict the results from exome sequence. Each line represents a distinct coverage read. Mean 20× coverage of all bases was above 82% for all patients. Each of these mutations induces a frame shift.

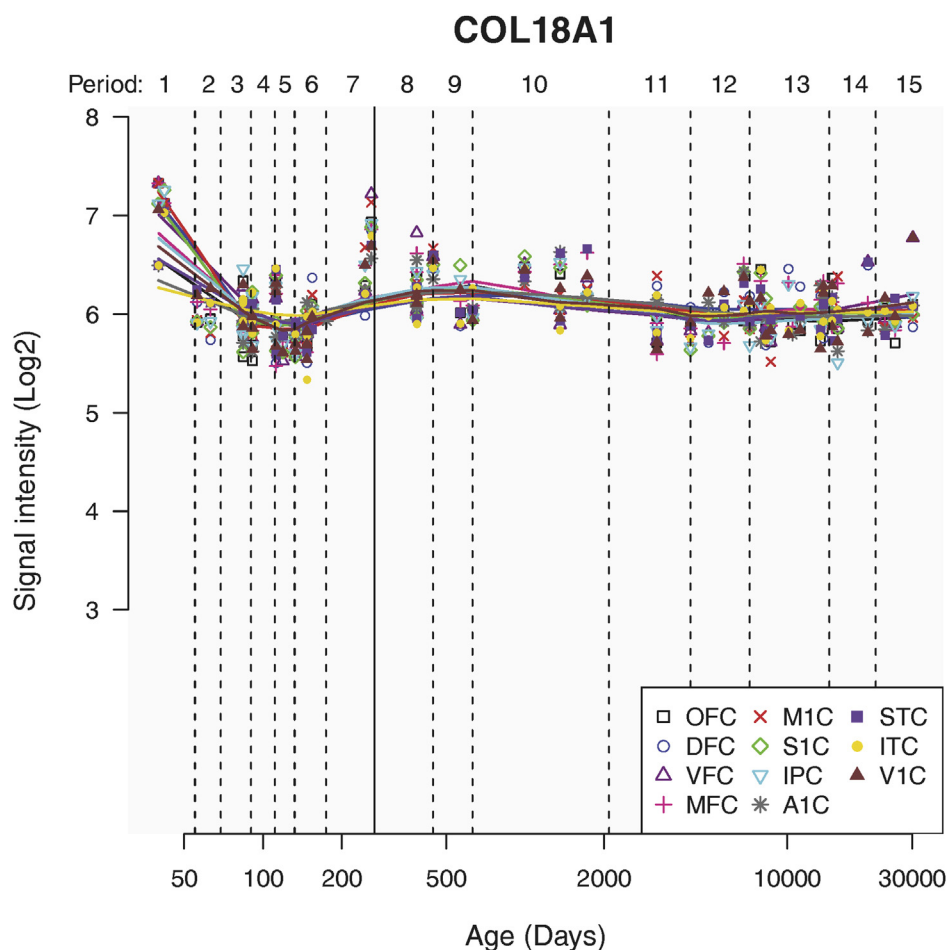
**SUPPLEMENTARY FIGURE 3.**

Chromatographs obtained via Sanger sequencing analysis of the three index patients analyzed via whole-exome sequencing (NG133-1, NG1348-1, and NG1426-1) and their siblings and parents. Note that the respective mutations identified via whole-exome sequencing were confirmed as homozygous mutations in the three index patients and their affected siblings and as heterozygous in their parents and unaffected siblings. DNA from healthy individuals was also Sanger sequenced, and these results are included as controls.



**SUPPLEMENTARY FIGURE 4.**

Representative chromatographs obtained via Sanger sequencing analysis of *COL18A1* patient (NG159-2) and her siblings and parents. Note that the identified mutation was homozygous in the patient and her affected siblings and as heterozygous in her parents and unaffected siblings. DNA from healthy individuals was also Sanger sequenced, and these results are included as controls. Also, please note that this mutation was identical to that identified in index patient NG133-1 (unrelated).

**SUPPLEMENTARY FIGURE 5.**

Trajectories of human COL18A1 expression in neocortical areas across development and adulthood. These data were obtained using the Human Brain Transcriptome database.<sup>21</sup> COL18A1 mRNA expression is low-to-moderate ( $6 < \log_2 \text{intensity} < 7$ ). The level of COL18A1 expression is highest during embryonic development (period 1), decreases during early-fetal and early mid-fetal development (periods 2-5), then starts to slightly rise from late mid-fetal development until infancy, and stays relatively constant at a low level throughout the rest of the postnatal timespan. A1C, primary auditory cortex; DFC, dorsolateral prefrontal cortex; IPC, inferior parietal cortex; ITC, inferior temporal cortex; M1C, primary motor cortex; MFC, medial prefrontal cortex; OFC, orbitofrontal prefrontal cortex; S1C, primary somatosensory cortex; STC, posterior superior temporal cortex; V1C, primary visual cortex; VFC, ventrolateral prefrontal cortex.

**SUPPLEMENTARY TABLE 1.**

Summary of Sequencing Quality Metrics Achieved by Whole-Exome Sequencing Performed on Three Index Patients (NG133-1, NG1348-1, and NG1426-1)

Patient ID	NG133-1	NG1348-1	NG1426-1
Number of lanes	1	1	1
Read Type (SR/PE)	PE	PE	PE
Read length	74	74	74
Total number of reads (millions)	98.4	73	84.6
Exome quality metrics			
% mapped to the exome	64.00	63.40	62.70
Mean target coverage	92.55	71.60	74.68
% of bases not covered	0.90	1.04	0.97
% of bases covered at least 20×	87	82	84
Duplicates (%)	4.61	3.17	3.14
Mismatches (%)	0.29	0.19	0.17

PE = paired end; SR = single read.

**SUPPLEMENTARY TABLE 2.**

Summary of Whole-Genome Genotyping and Whole-Exome Sequencing Results for Index Patient NG133-1

Blocks of Shared Homozygosity							
Chr	Start	End	SNP Start	SNP End	Number of SNPs	Length (cM)	Length (Mb)
4	79229609	89149570	rs12505887	rs9307048	410	9.7	9,919,961
7	32440555	37344369	rs369052	rs2723996	247	5.49	4,903,814
12	126290697	128392360	rs2079548	rs1488144	163	6.28	2,101,663
14	49966883	56336645	rs8017939	rs945272	378	7.6	6,369,765
17	13292146	17715101	rs7220603	rs11868035	303	9.32	4,422,955
21	43801075	48084747	rs2251362	rs15047	355	7.4	4,235,031
Total					1856	46	31,953,189
Novel Homozygous Variants Identified Within the Shared Homozygosity Intervals							
Chr	Position	Base Change	Gene	Mutation Type	Existing Variation	Amino Acid Change	GERP_BASE
14	51347189	C>G	<i>ABHD12B</i>	Missense	rs141865189	p.Arg119Gly	0.868
21	46930004	CT	<i>COL18A1</i>	Deletion	None	p.Leu1590ValfsX72	3.44

Abbreviations:

Chr = Chromosome

SNP = Single nucleotide polymorphism

Mb = Million base pairs

Blocks of genomic homozygosity were identified via whole-genome genotyping. Homozygous variants were identified via whole-exome sequencing.

**SUPPLEMENTARY TABLE 3.**

Summary of Whole-Genome Genotyping and Whole-Exome Sequencing Results for Index Patient NG1348-1

Blocks of Shared Homozygosity							
Chr	Start	End	SNP Start	SNP End	Number of SNPs	Length (cM)	Length (Mb)
1	37773050	43741713	rs7516603	rs2991996	277	7.27	5,968,663
1	10767902	14808756	rs488834	rs2480061	231	8.7	3,990,854
1	153456349	164440415	rs12025638	rs12723400	681	14.14	10,984,066
1	83014374	98667546	rs318405	rs822555	805	15.23	15,653,172
1	1005806	9704925	rs3934834	rs4129341	600	18.61	8,631,843
2	225003290	235502345	rs6752059	rs940947	710	15.73	10,455,550
3	93883640	133877570	rs6805571	rs4854617	1939	36.02	39,993,930
4	186801590	190872778	rs4343763	rs12646565	318	9.61	4,071,188
6	168533451	169778429	rs1565441	rs9283855	118	2.77	1,244,054
7	78319728	111617978	rs7791589	rs3852333	1527	31.45	33,247,550
21	43493586	48084747	rs220281	rs15047	403	8.28	4,542,520
Total					7609	168	138,783,390
Novel Homozygous Variants Identified Within the Shared Homozygosity Intervals							
Chr	Position	Base Change	Gene	Mutation Type	Existing Variation	Amino Acid Change	GERP_BASE
1	1,354,884	C>T	<i>ANKRD65</i>	Missense		p.Asp266Asn	4.22
1	12,034,846	T>C	<i>PLOD1</i>	Missense		p.Val769Ala	5.69
1	156,347,149	T>G	<i>RHBG</i>	Missense	TMP_ESP_1_156347149	p.Leu82Arg	5.06
1	91,403,290	A>G	<i>ZNF644</i>	Missense	Rs138567555	p.Leu1147Pro	6.06
2	233,410,311	T>C	<i>CHRNA3</i>	Missense		p.Met480Thr	4.53
3	111,697,931	C>A	<i>ABHD10</i>	Missense	rs142771529	p.Ala8Asp	4.2
3	100,523,692	C>G	<i>ABI3BP</i>	Missense	rs146922324	p.Arg142Pro	-8.04
3	120,315,290	A>T	<i>NDUFB4</i>	Missense		p.Glu28Asp	1.34
3	101,384,086	T>A	<i>ZBTB11</i>	Missense	rs151249814	p.Ser449Cys	3.02
7	80,300,413	C>A	<i>CD36</i>	Stop gained		p.Cys274X	2.81
7	51,092,945	G>A	<i>COBL</i>	Missense	rs200941312	p.Pro1210Leu	1.57
7	94,058,557	A>G	<i>COL1A2</i>	Missense		p.Met1257Val	5.09
7	102,108,740	C>G	<i>LRWD1</i>	Missense	rs148425285	p.Leu279Val	4.17
21	46,897,722	G>GC	<i>COL18A1</i>	Frame shift		p.Gly773ArgfsX55	0.55
21	45,175,839	C>T	<i>PDXK</i>	Missense	rs146321963	p.Pro256Leu	-6.04
X	135,405,024	G>A	<i>GPR112</i>	Missense	rs145927330	p.Ser53Asn	0.501
X	2,777,906	G>A	<i>GYG2</i>	Missense		p.Val244Ile	3.73
X	106,198,144	T>C	<i>MORC4</i>	Missense		p.Ser310Gly	5.46
X	153,689,016	C>G	<i>PLXNA3</i>	Missense		p.Leu165Val	3.19

Abbreviations:

Chr = Chromosome

SNP = Single nucleotide polymorphism

Mb = Million base pairs

Blocks of genomic homozygosity were identified via whole-genome genotyping. Homozygous variants were identified via whole-exome sequencing.

**SUPPLEMENTARY TABLE 4.**

Summary of Whole-Genome Genotyping and Whole-Exome Sequencing Results for Index Patient NG1426-1

Blocks of Shared Homozygosity							
Chr	Start	End	SNP Start	SNP End	Number of SNPs	Length (cM)	Length (Mb)
1	210749312	215816688	rs12567982	rs2677111	256	5.4	5,067,376
2	9290324	10469516	rs1344185	rs1003653	95	2.81	1,179,192
3	38541318	45154868	rs2300669	rs4683045	262	5.32	6,613,550
3	9568136	24758368	rs9846242	rs4858125	969	20.64	15,190,236
4	54559738	62693692	rs2590783	rs11734607	358	10.03	8,121,792
4	79229609	129024273	rs12505887	rs4834232	1914	42.01	49,795,090
9	90137616	93843942	rs871495	rs296636	260	5.63	3,556,327
10	135853	4037207	rs7906287	rs11252249	320	8.59	3,901,354
11	119677072	121779664	rs895648	rs747915	152	4.08	2,102,592
12	193818	3992311	rs4980929	rs10774180	317	9.24	3,798,493
12	5022438	10176144	rs4766311	rs10505745	350	10.07	5,174,712
12	79911687	93653808	rs1553525	rs10777489	498	10.85	13,742,121
13	47403360	53474967	rs7333412	rs4460964	294	5.01	6,071,607
14	86658674	94336880	rs8022696	rs12895705	460	11.08	7,678,206
15	98006502	102388692	rs4965192	rs1355871	315	12.33	4,398,709
16	52675052	54403388	rs6498990	rs7206352	102	3.76	1,728,336
16	17896645	24046568	rs4780669	rs3785383	239	8.95	6,149,923
18	18609580	22118315	rs288980	rs1791520	140	2.81	3,508,735
18	71704019	73518619	rs9961095	rs1460273	131	3.81	1,792,608
18	2634848	15082789	rs9303909	rs1852893	866	33.99	12,447,941
20	11046619	19762648	rs6104699	rs9653629	649	15.28	8,716,029
20	222632	6994830	rs12624551	rs6133387	641	21.67	6,772,198
21	45978898	48084747	rs170847	rs15047	170	3.59	2,105,849
Total					9758	257	179,612,976
Novel Homozygous Variants Identified Within the Shared Homozygosity Intervals							
Chr	Position	Base Change	Gene	Mutation Type	Existing Variation	Amino Acid Change	GERP_BASE
1	214557615	G>A	<i>PTPN14</i>	Missense	rs141184727	p.Pro528Leu	4.45
14	91804426	C>A	<i>CCDC88C</i>	Missense	rs200244690	p.Val325Leu	5.36
21	45756674	TGCC	<i>COL18A1</i>	Insertion	None	p.Ala1734CysfsX14	0.598

Abbreviations:  
Chr = Chromosome  
SNP = Single nucleotide polymorphism  
Mb = Million base pairs

Blocks of genomic homozygosity were identified via whole-genome genotyping. Homozygous variants were identified via whole-exome sequencing.

**SUPPLEMENTARY TABLE 5.**

List of the Top 100 Genes With Expression Patterns That Are Positively Correlated With *COL18A1* Expression

Rank	Gene	Correlation to <i>COL18A1</i>	Rank	Gene	Correlation to <i>COL18A1</i>
1	<i>COL18A1</i>	1.00	51	<i>TGDS</i>	0.58
2	<i>RBPMS</i>	0.70	52	<i>GATA2</i>	0.58
3	<i>SMAD6</i>	0.69	53	<i>SILV</i>	0.58
4	<i>BCAM</i>	0.69	54	<i>DPPA4</i>	0.58
5	<i>DOCK6</i>	0.69	55	<i>MOV10</i>	0.58
6	<i>MECOM</i>	0.69	56	<i>XKRX</i>	0.58
7	<i>F10</i>	0.68	57	<i>CD248</i>	0.58
8	<i>ID3</i>	0.68	58	<i>TCF7</i>	0.58
9	<i>COL6A3</i>	0.68	59	<i>FAP</i>	0.58
10	<i>EMCN</i>	0.68	60	<i>C1ORF106</i>	0.57
11	<i>SIX4</i>	0.67	61	<i>TNFAIP8</i>	0.57
12	<i>VEGFC</i>	0.66	62	<i>PLCD1</i>	0.57
13	<i>LAMC3</i>	0.65	63	<i>SRPX2</i>	0.57
14	<i>ERG</i>	0.65	64	<i>XPNPEP2</i>	0.57
15	<i>TCP11</i>	0.64	65	<i>C6ORF150</i>	0.57
16	<i>ATP8B3</i>	0.64	66	<i>KANK2</i>	0.57
17	<i>ADCY4</i>	0.63	67	<i>GUCY2E</i>	0.57
18	<i>TGFB1</i>	0.63	68	<i>RARG</i>	0.57
19	<i>RREB1</i>	0.63	69	<i>EGFL7</i>	0.57
20	<i>BCL2L12</i>	0.62	70	<i>FOXD1</i>	0.57
21	<i>KLHL6</i>	0.62	71	<i>NPR1</i>	0.57
22	<i>SLC16A3</i>	0.62	72	<i>PCGF6</i>	0.57
23	<i>NOD1</i>	0.61	73	<i>BAIAP2L1</i>	0.57
24	<i>C1ORF97</i>	0.61	74	<i>CCND1</i>	0.57
25	<i>NFKB2</i>	0.61	75	<i>ST6GALNAC1</i>	0.57
26	<i>CLEC1A</i>	0.61	76	<i>C1QTNF7</i>	0.57
27	<i>SPTA1</i>	0.61	77	<i>IMPA2</i>	0.57
28	<i>SELP</i>	0.60	78	<i>ADSSL1</i>	0.57
29	<i>ATF3</i>	0.60	79	<i>HIST1H2AM</i>	0.57
30	<i>ALPK3</i>	0.60	80	<i>TRIM56</i>	0.56
31	<i>THBD</i>	0.60	81	<i>SLFN13</i>	0.56
32	<i>MECOM</i>	0.60	82	<i>TEAD3</i>	0.56
33	<i>LSR</i>	0.60	83	<i>ACTG2</i>	0.56
34	<i>TGFB1</i>	0.60	84	<i>LSP1</i>	0.56
35	<i>GDF15</i>	0.60	85	<i>XKR5</i>	0.56
36	<i>FHOD1</i>	0.60	86	<i>PLCB3</i>	0.56
37	<i>PLVAP</i>	0.60	87	<i>REEP4</i>	0.56
38	<i>CDH5</i>	0.60	88	<i>CPZ</i>	0.56
39	<i>PHF10</i>	0.60	89	<i>PLA2G3</i>	0.56
40	<i>RHBDF1</i>	0.59	90	<i>SLC43A1</i>	0.56
41	<i>ID1</i>	0.59	91	<i>SDPR</i>	0.56
42	<i>MXRA8</i>	0.59	92	<i>RBPMS2</i>	0.56
43	<i>RHAG</i>	0.59	93	<i>MGMT</i>	0.56
44	<i>SYDE1</i>	0.59	94	<i>SBNO2</i>	0.56
45	<i>PLBD1</i>	0.59	95	<i>SLC2A1</i>	0.56
46	<i>ITGA5</i>	0.59	96	<i>EDN3</i>	0.56
47	<i>MALL</i>	0.58	97	<i>C7ORF10</i>	0.56
48	<i>CHMP4C</i>	0.58	98	<i>CYR61</i>	0.55
49	<i>SLC26A6</i>	0.58	99	<i>XRCC3</i>	0.55
50	<i>CRIP1</i>	0.58	100	<i>TNFRSF1A</i>	0.55

Three genes that are known to cause cortical malformation syndromes are bolded (*DOCK6*, *COL6A3*, and *LAMC3*).